J Mater Sci (2008) 43:1444–1450
DOI 10.1007/s10853-007-2312-4

Effect of grain size on the primary and secondary creep behavior of Sn–3 wt.% Bi alloy

Alaa Farag Abd El-Rehim

Received: 2 January 2007 / Accepted: 12 November 2007 / Published online: 12 December 2007

Abstract The effect of grain size as well as creep temperature on the primary and secondary creep parameters of Sn–3 wt.% Bi alloy has been studied. It was found that the creep parameters α, β, and $\dot{\varepsilon}_s$ were decreased with increasing grain size. This was explained in view of the dislocation interaction with the defects and different inclusions in the matrix. For both the primary and secondary creep, the activation energies estimated indicate that the rate-controlling mechanism is the grain boundary-sliding mechanism.

Introduction

Based on the increasing pressure to achieve environmentally friendly electronic materials and processes, and indeed, growing governmental regulations around the world, there is a strong drive to use lead-free solders in electronic assemblies [1–3]. Requirements for the new solder materials include environment friendliness, compatibility with the existing manufacturing line, good wettability, good mechanical and electrical properties, and low cost, among others. Recently, the use of binary Sn–Bi solder alloys [4–6] has been gaining wide support from the industry, but data on their mechanical properties are rare.

Grain size is one of the most important variables characterizing the microstructure of polycrystalline materials. Grain-boundary movement plays an important role in the work-hardening characteristics [7, 8]. When different grain sizes are prepared with a minimum grain growth, leading to random distribution of grain-boundary misorientation, the secondary creep rate, $\dot{\varepsilon}_s$, should increase with increasing grain size [9]. This is attributed to decrease of boundary barriers with increasing grain size. On the other hand, when different grain sizes are produced by grain growth method, $\dot{\varepsilon}_s$ should decrease with increasing grain size. This is because the large grain size samples are poor sources of vacancies, leading to a low dislocation climb rate.

The same author [10] studied the creep characteristics of Sn–3 wt.% Bi alloy under different applied stresses ranging from13.24 to 16.30 MPa and at different testing temperatures ranging from 300 to 370 K. The observed results indicated that a transition in the creep behavior occurs at a testing temperature $\sim$330 K. The variation in the creep parameters n, β, and $\dot{\varepsilon}_s$ with increasing testing temperature was explained on the basis of coarsening and dissolution of β-phase (Bi-rich phase) occurring in Sn–Bi alloys. On the other hand, Saad et al. [11] studied the grain size dependence of creep properties of Sn–0.5 at.% Bi alloy by using samples of various grain sizes in the stress range 24.7–32.5 MPa. It was found that the secondary creep rate decreased by increasing grain size. This was interpreted as being due to the segregation of the solute atoms (Bi) in the vicinity of the grain boundaries as well as on the moving dislocations. It was reported [12] that pretorsional deformation has considerable effect on the secondary creep rate of polycrystalline Sn–0.5 at.% Bi alloy. Low degrees of pretorsional deformation decreased the secondary creep rate to a minimum followed by an increase at higher degrees of deformation. The critical degree of pretorsional deformation corresponding to the minimum secondary creep rate was found to depend on the creep temperature as well as on the applied stress. The results were interpreted on the basis of dislocation density and stability of preinduced substructures.

A. F. Abd El-Rehim (✉)
Physics Department, Faculty of Education, Ain Shams University, P.O. Box 5101, Heliopolis 11771, Roxy, Cairo, Egypt
e-mail: afabdelrehim@yahoo.com

Alden [13] studied the plastic deformation processes in an extruded Sn-5 wt.%Bi alloy by means of mechanical measurements and microstructure observations, and concluded that the flow stress and strain-rate sensitivity of the flow stress are strong functions of both strain-rate and Sn-grain size. Pattanaike and Raman [14] had made a series of experiments on Sn–Bi solder in an attempt to characterize its mechanical behavior including tensile tests over different ranges of strain-rates and the steady state stresses, and to obtain a relation between them.

Secondary creep of Sn–1 wt.%Bi, Sn–2 wt%Bi, and Sn–5 wt% Bi as a function of stress and temperature was studied by Milten et al. [15], and they obtained an empirical equation to show the linear dependence at low strain rate and an exponential stress dependence at high strain rate. Their observations suggested that dislocation climb was the active mechanism in the nonlinear region. They also found that the stress sensitivity of the secondary creep was similar to that of pure "Sn", and the addition of "Bi" had decreased the secondary creep rates.

The activation energies for secondary creep in the Sn–5 wt.%Bi alloy were studied by Al-Ganainy et al. [16] in the vicinity of the transformation temperature (328 K) and above it and found to be 62 and 87 KJ/mole, respectively, and characterized them by the grain-boundary-sliding (G.B.S.) mechanism. The same authors [17] studied the secondary creep in the case of Sn–1 wt.%Pb alloy in low and high ranges of temperatures and obtained the activation energies with values of 37.2 and 57 KJ/mole, respectively, and explained these values again by grain-boundary-sliding-mechanism.

The understanding of a material's response to deformation conditions is vital in order to predict the microstructural development during industrial forming processes [18]. Because of the lack of information about the effect of grain size on its creep parameters, the aim of this work is to investigate the effect of grain size and creep temperature on the creep behavior of Sn–3 wt.% Bi alloy.

Experimental procedure

Sample preparation

The elements used to prepare the alloy in this study are Sn and Bi of 99.99% purity. They were weighted and well mixed with $CaCl_2$ flux to prevent oxidation in a graphite crucible and chill casting. The cast rod was homogenized by annealing at 423 K for 24 h, then swaged in wire form of diameter 0.5 mm. Samples of different grain sizes were obtained by annealing four groups of samples for 1 h at different temperatures in the solid solution region ranging from 353 to 413 K and then quenched in water to room temperature (300 K). To reveal the grain boundaries, samples were treated for a few seconds with 2 vol.% Hydrochloric acid in ethanol as enchant. The average grain size for each group was determined by using the line intercept method. The average grain sizes obtained were 26, 32, 48, and 110 μm for annealing temperatures of 353, 373, 393, and 413 K, respectively.

Tensile creep measurements

Constant load creep uniaxial tests were conducted using a convenient creep machine equipped with a length dial gauge of a sensitivity of 10^{-4} cm. The creep tests have been performed under constant load corresponding to a stress of 18.32 MPa and at different creep temperatures, T, of 303, 313, 323, and 333 K. The accuracy of temperature measurements is of the order of ±1 K.

Experimental results

Creep curves of strain as a function of time of Sn–3 wt.% Bi alloy samples of different grain sizes 26, 32, 48, and 110 μm obtained under a constant stress of 18.32 MPa and at different creep temperatures ranging from 303 to 333 K in steps of 10 K are shown in Fig. 1. The creep curves show three distinct stages: primary creep where the strain rate decreases with time, secondary creep with a constant strain rate, and lastly, tertiary creep where the strain rate accelerates to fracture [19].

It was found that the primary creep obeys the equation [20, 21]:

$$\varepsilon_{pr} = \beta t^{\alpha} \quad (1)$$

where α and β are the primary creep parameters and t is the primary creep time in seconds. The parameters α and β are correlated from the relation between ln ε_{pr} and ln t at different creep temperatures for various grain sizes. α and β are determined from the slopes and the intercepts of the straight lines in Fig. 2, respectively. Figure 3 represents the grain size, d, dependence of the parameters α and β. They are found to exhibit values ranging from (0.29–0.85) for α and (1.93–23.50) $\times$ 10^{-4} for β.

The secondary creep rate, ε'_s, values were evaluated from the linear parts of the creep curves of Fig. 1. Figure 4 illustrates the secondary creep rate, ε'_s, as a function of the grain size, d, from which it is clear that ε'_s decreases with increasing grain size, d, and increases with increasing creep temperature, T.

The activation energy of the primary creep stage, Q_{pr} (in kJ/mol), is calculated using the following equation [22]:

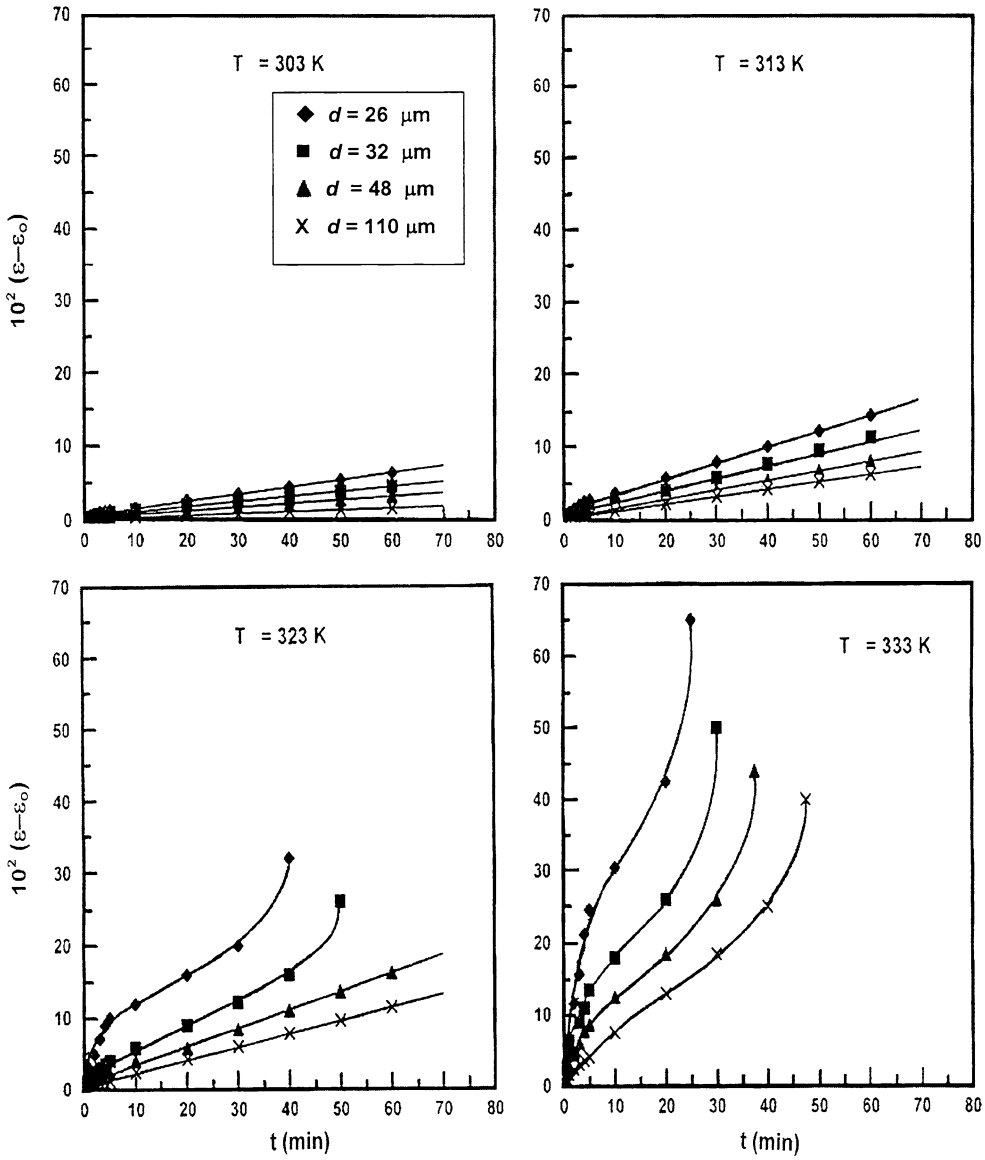

Fig. 1 Creep curves for Sn–3 wt.% Bi wires with different grain sizes and creep temperatures as indicated (ε_o is instantaneous creep at time = 0)

$$\beta = \text{constant } \exp(-Q_{pr}/k\mathrm{T}) \quad (2)$$

where k is Boltzmann's constant. The slopes of straight lines relating ln β and 10^3/T (K^{-1}) (Fig. 5) yield an activation energy of a mean value of ~67 kJ/mol for primary creep stage.

While the values of ε'_s satisfy the equation [23]:

$$\varepsilon'_s = \text{constant } \exp(-Q_s/k\mathrm{T}) \quad (3)$$

where Q_s is the activation energy of the secondary creep stage (in kJ/mol). Figure 6 illustrates the relation between ln ε'_s and 10^3/T (K^{-1}). The slopes of these straight lines yield activation energy of a mean value of ~72 kJ/mol for secondary creep stage.

Discussion

The primary creep was observed in almost all low-stress creep experiments even if the main attention was paid to secondary state mostly. Since some mechanisms assumed to be responsible for creep deformation in secondary stage are not capable to explain the primary creep, special primary creep mechanisms must be taken into account. Better understanding of these mechanisms seems to be important for engineering practice since the overall strain allowed for some components in high-temperature technology may be essentially exhausted during the primary creep stage duration.

The parameter α determines the dependence of the mobile dislocation density, τ, on the value of the mean

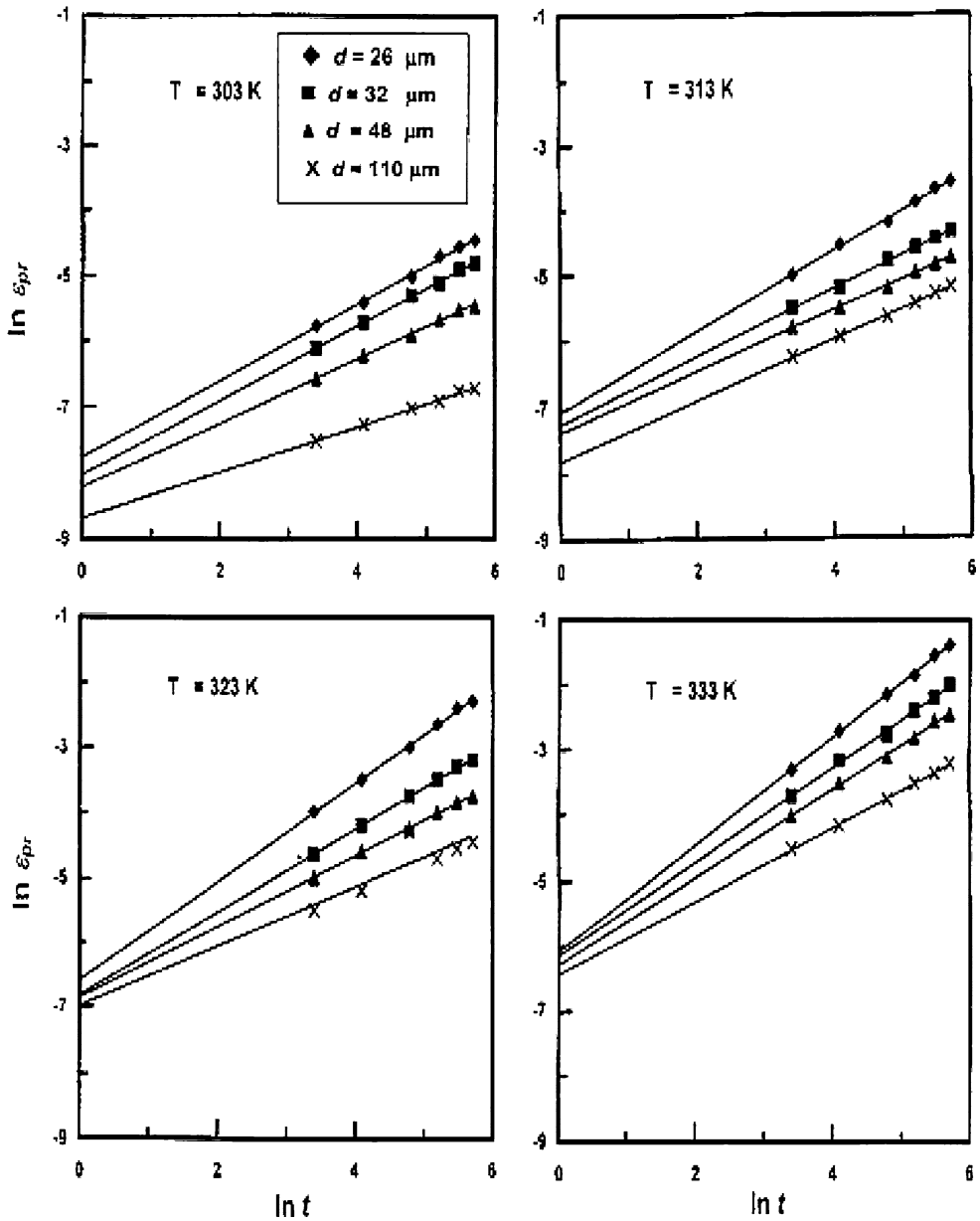

Fig. 2 Relation between ln ε_{pr} and ln t for Sn–3 wt.% Bi wires with different grain sizes and creep temperatures as indicated

internal stress, σ_i, and relaxed shear modulus G [9, 24] according to the relation:

$$\tau = \sigma_i^2/(\alpha G b)^2 \quad (4)$$

where b is Burgers vector of the dislocations involved. If we follow the assumption [24, 25] that the mobile dislocation density is a constant fraction of the total density and take into consideration that increasing grain size results in a decrease in σ_i, the decrease of α with increasing of grain size (Fig. 3a) could be accounted for. This behavior is consistent with other experimental data reported in the literature [9, 11].

The observed decrease in β with increasing grain size (Fig. 3b) at a constant stress in the whole creep temperature range could be explained on the basis that Bi in solid solution is homogeneously distributed on dislocations and has a strong influence on their thermal glide in the grain interior. As the grain size increases during the annealing process, some of the Bi atoms will disperse near the Sn grain-boundary regions and pin mobile dislocations [26]. This increases strengthening and limits grain boundary motion. This is consistent with the commonly, reported [14] effect of alloying elements, which act principally to refine and stabilize the Sn grains size and are more effective in large concentrations. This eventually impedes the motion of the dislocations; consequently the parameter β decreases.

Figure 4 shows the relationship between the secondary creep rate, ε'_s, and the grain size at different creep temperatures. This grain size refinement is usually carried out

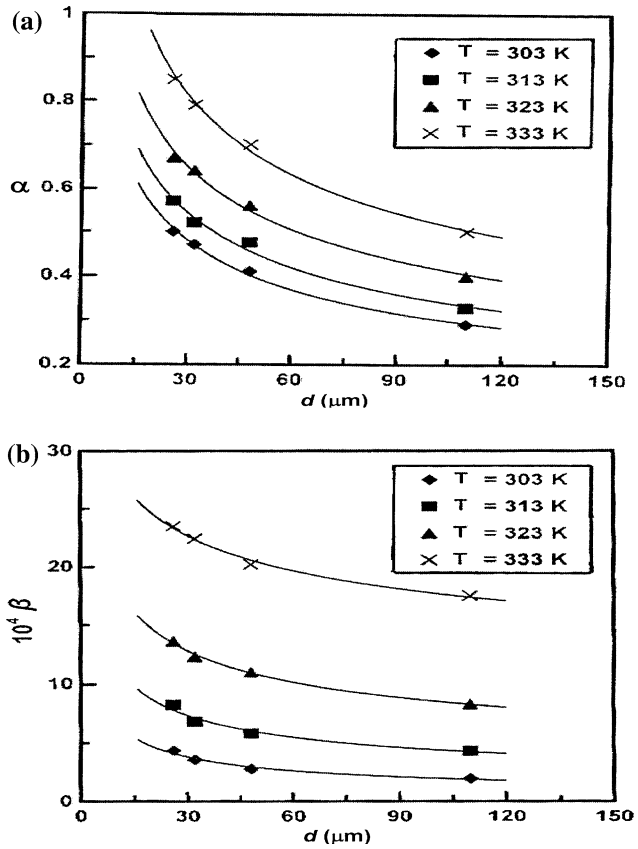

Fig. 3 The grain size, d, dependence of the primary creep parameters (**a**) α, and (**b**) β, at different creep temperatures as indicated

by thermomechanical treatment that produces fine, hard, dispersed particles (Bi atoms) that pin the grain boundary and retard the tendency of strain-enhanced grain growth during the deformation [27]. In such a microstructure, intragranular Bi particles would hinder the movement of lattice dislocations from passing from one side of the grain

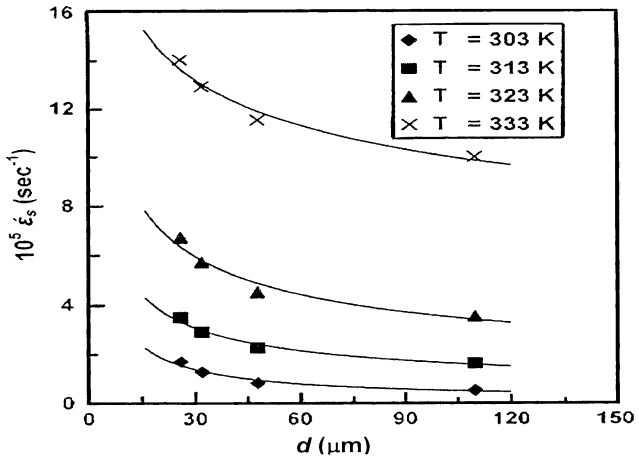

Fig. 4 Dependence of the secondary creep rate ε'_s on the grain diameter, d, at different creep temperatures as indicated

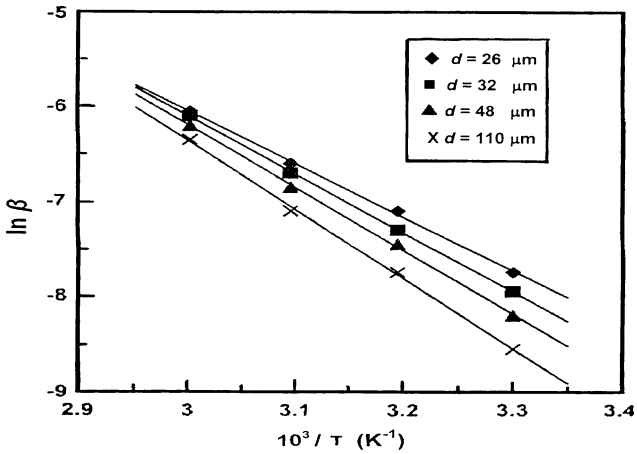

Fig. 5 Relation between ln β and 10^3/T at different grain sizes as indicated

to the other side, thereby making the slip-related accommodation step during deformation difficult. Furthermore, the intergranular particles will directly influence grain-boundary sliding (GBS) by acting as barriers to sliding. Consequently, ε'_s will decrease by increasing grain size.

The secondary creep rate, ε'_s, is related to the grain size, d, by the Mukherjee–Bird–Dorn equation [28]:

$$\varepsilon'_s = A\frac{DGb}{kT}\left(\frac{\sigma}{G}\right)^n\left(\frac{b}{d}\right)^p \tag{5}$$

where A is a constant which depends on the material and the dominant deformation mechanism (mechanistic constant), σ is the applied stress, D is the appropriate diffusion coefficient ($=D_0\exp(-Q_{app}/RT)$, D_0 being a frequency factor, R the gas constant, and Q the activation energy for the deformation process), p is the grain size exponent, n is the stress exponent. At constant applied stress, Eq. 5 prescribes a linear relationship in logarithmic coordinates between the secondary creep rate, ε'_s, and grain size, d, for a specified creep temperature. Figure 7 shows the

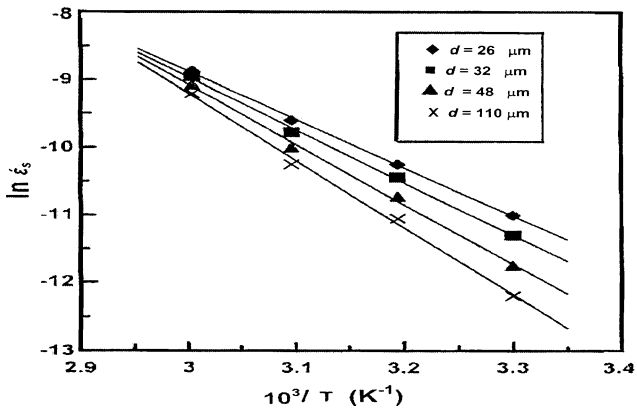

Fig. 6 Relation between ln ε'_s and 10^3/T at different grain sizes as indicated

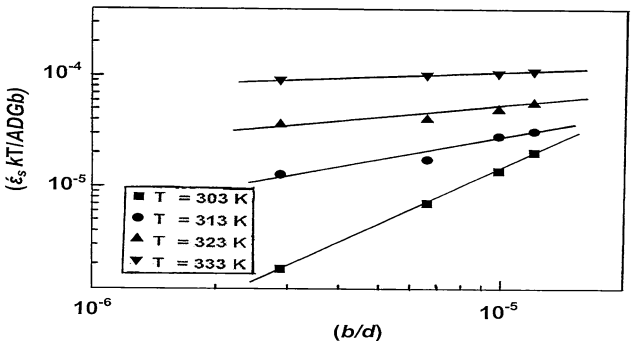

Fig. 7 A double-logarithmic plot of normalized secondary creep rate versus normalized grain size for various constant creep temperatures

relationship between the normalized secondary creep rate and the normalized grain size (both on logarithmic scales) at different constant creep temperatures. The slope of each line fitted to the data gives the grain size exponent, p. The mean value of p was found to be ≈ 2. The present value of p is in good agreement with those reported previously [29–31]. When the secondary creep rate dependence on grain size with the reciprocal of grain size is squared, the deformation creep process is that of grain-boundary sliding accommodated by slip [32].

The activation energy (67 kJ/mol) for primary creep was approximate to that for the secondary creep (72 kJ/mol). These values of activation energy indicate that the primary creep, as well as the secondary creep, was controlled by grain-boundary sliding as the dominant operating mechanism [10, 15, 16].

Since creep is a continuous process, the primary creep ε_{pr} represented by Eq. 1 strongly influences the secondary creep rate, ε'_s, obtained from the relation [33]:

$$\beta = \beta_o \, (\varepsilon'_s)^{\gamma} \tag{6}$$

where β_o is a constant and γ is the secondary creep exponent measuring the contribution of the primary creep

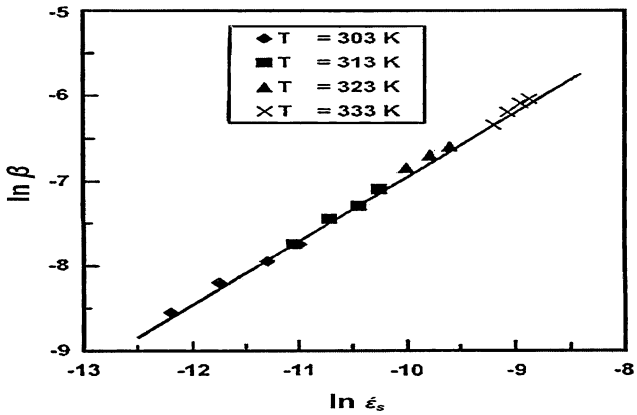

Fig. 8 Relation between ln β and ln ε'_s at different creep temperatures as indicated

mechanism to the secondary creep behavior. The relation between ln β and ln ε'_s as in Fig. 8 yielded a straight line with an average value of $\gamma = 0.77$. This relatively high value of γ confirms again that the mechanism responsible for the primary creep stage also operates in the secondary creep stage.

Conclusions

This study is being conducted to determine the influence of grain size on the creep behavior of Sn–3 wt.% Bi alloy and the following results were obtained from this study:

- The creep parameters α, β, and ε'_s were found to be increased with increasing creep temperature, while they decreased with increasing grain size.
- Increasing grain size in the temperature range 303–333 K leads to a significant increase in the strength and improvement in the creep resistance.
- The calculated activation energy values indicated that the dominant creep mechanism is the grain-boundary sliding.

References

1. Gao KF, Takemoto T, Nishikawa H (2006) Mater Sci Eng A 420:39
2. Zeng K, Tu KN (2002) Mater Sci Eng Rep 38:55
3. Shin SW, Yu J (2003) Jpn J Appl Phys 42:1368
4. Song HG, Morris JW, Hua F (2002) Mater Trans A 43:1847
5. Hua F, Mei Z, Glazer J (1998) Proceedings 48th electronics components and technology conference, May 25–28, Seattle, pp 277–283
6. Mei Z, Morris JW (1992) J Electron Mater 21:599
7. Fawzy A, Nada RH (2006) Physica B 371:5
8. Van Swygenhoven H, Spaczer M (1999) Phys Rev B 60:22
9. Saad G, Graiss G, Fawzy A, Kenawy MA (1991) Ind J Pure Appl Phys 29:344
10. Abd El-Rehim AF (2007) J Alloys Compd 440:127
11. Saad G, Abd El-Salam F, Mostafa MT (1984) Surf Technol 22:73
12. Kenawy MA, Saad G, Mostafa MT (1983) Solid State Commun 46:763
13. Alden TH (1967) Acta Metall 15:469
14. Pattanaike S, Raman V (1991) IBM conference: material development in microelectronic packaging, performance and reliability. Montreel, Quebec
15. Miltin D, Raedu CH, Messlar RW (1999) J Metall Mater Trans A 30:115
16. Al-Ganainy GS, Nagy MR, Khalifa BA, Afify R (1996) Phys Status Solidi A 158:463
17. Al-Ganainy GS, Nagy MR, Khalifa BA, Afify R (2002) Egypt J Sol 25:1
18. Van Geertruyden WH, Misiolek WZ, Wang PT (2006) Mater Sci Eng A 419:105
19. Nabarro FRN, de Villiers HL (1995) The Physics of creep. Taylor and Francis, London
20. Abd El-Rehim AF (2007) Mater Sci Technol 23:620

21. Wilshire B, Evans RW (1985) Creep behaviour of crystalline solids. Pineridge press Ltd., Swansea, p 34
22. Mahmoud MA, Abd El-Rehim AF, Abd El-Khalek AM, Ashry AH, Graiss G (2005) Cryst Res Technol 40:665
23. Kenawy MA, Sakr MS, Sakr EM, Zayed HA, Mourad NO (1990) Phys Stat Solidi A 121:467
24. Youssef SB, Fawzy A, Sobhy M, Saad G (1995) Cryst Res Technol 30:7
25. Kassner ME (1993) Mater Sci Eng A 166:81
26. Al-Ganainy GS, Mostafa MT (2000) Egypt J Sol 23:333
27. Mukherjee AK (2002) Mater Sci Eng A 322:1
28. Mukherjee AK, Bird JE, Dorn JE (1969) Trans Am Soc Metals 62:155
29. Yamane T, Genma N, Takahashi T (1984) J Mater Sci 19:263. doi 10.1007/BF00553017
30. Schneibel J, Hazzledine P (1983) J Mater Sci 18:562. doi 10.1007/BF00560645
31. Mahamed FA, Langdon TG (1975) Phil Mag A 32:697
32. Wadsworth J, Ruano OA, Sherby OD (2002) Metall Mater Trans A 33:219
33. Abd El-Salam F, Abd El-khalekh AM, Nada RH (2000) Eur Phys J AP 12:159